ESD-TR-69-159

Semiannual Technical Summary

Seismic Discrimination

30 June 1969

Lincoln Laboratory

MASSACHUSETTS INSTITUTE OF TECHNOLOGY

Lexington, Massachusetts

AD0691434

MASSACHUSETTS INSTITUTE OF TECHNOLOGY

LINCOLN LABORATORY

SEISMIC DISCRIMINATION

SEMIANNUAL TECHNICAL SUMMARY REPORT
TO THE
ADVANCED RESEARCH PROJECTS AGENCY

1 JANUARY – 30 JUNE 1969

ISSUED 29 JULY 1969

LEXINGTON   MASSACHUSETTS

ABSTRACT

Seismic source identification work during this reporting period
has emphasized continued studies of short-period discriminants;
in particular, the physical sources of some of the spectral ef-
fects observed, attempts to exploit arrays of several thousand
kilometers' aperture, and a probabilistic model of the two cur-
rently most promising discriminants.

CONTENTS

SUMMARY

This is the eleventh Semiannual Technical Summary of Lincoln Laboratory's work for the Advanced Research Projects Agency on the seismic discrimination problem (Vela Uniform).

We continue to devote attention to short-period P-wave spectral characteristics as a promising avenue for decreasing the present identification threshold. Recent work has concentrated on studies of the Q-factor (losslessness) of the mantle near the LASA (Montana) and NORSAR (Norway) receiving sites, since Q has a controlling effect on the visibility of explosion-earthquake spectral differences at any observing site. A suitable spectral ratio discriminant for NORSAR P-waves has been developed and tested and a theoretical model of explosion sources has been used to infer mantle Q for NORSAR (Sec. I-A). Comparison of NORSAR and Montana P-spectra of the same earthquakes has been used to compare the mantle Q for the two locations (Sec. I-B).

A systematic examination has been made of the usefulness of a continental array consisting of coherently combined seismometers spread over an aperture of several thousand kilometers (Sec. I-C). The hoped-for improvements in depth phase detectability and in resolution of the directional properties of the arriving P-coda were not realized, presumably due to large inter-site differences in crustal structure which proved impossible to equalize.

The usefulness of the surface wave vs body wave (M_s vs m_b) discriminant depends on good knowledge of the surface wave arrival time, particularly when other events may interfere. A brief study of the reliability of arrival time observations at LASA is reported in Sec. I-D.

An analysis has been completed of the probability, as a function of magnitude, of successfully applying either or both of two discriminants at LASA, M_s vs m_b and spectral ratio (Sec. I-E). This information is required for system studies of the identification problem.

The derivation of a seismicity recurrence curve from a large data population and its interpretation in terms of detection threshold is analyzed as a parameter estimation problem in Sec. II-A. Section II-B describes recent experiments in discerning migrational trends in successive earthquake epicenters using computer generated movies.

The laser interferometer strain measurement project has yielded interesting new information on atmospheric fluctuations which are described in Sec. II-C.

Section II-D discusses current status of the signal processing hardware and software in our new Cambridge facility being shared with the Earth and Planetary Sciences Department.

P. E. Green, Jr.

GLOSSARY

ARPA	Advanced Research Projects Agency
LASA	Large Aperture Seismic Array, Billings, Montana
LP	Long Period
LRSM	Long Range Seismic Measurements
MACFLAP	Macro Version of Fleck's Assembly Program
MSR	Modified Spectral Ratio
NORSAR	Norwegian Seismic Array
SATS	Semiannual Technical Summary
SNR	Signal-to-Noise Ratio
SP	Short Period
TFSO	Tonto Forest Seismic Observatory
USCGS	United States Coast and Geodetic Survey

SEISMIC DISCRIMINATION

I. IDENTIFICATION

A. SHORT-PERIOD SEISMIC SPECTRUM AT NORSAR

A detailed study of the short-period seismic spectrum at the NORSAR large aperture array in Norway is in progress. The following is a discussion of the spectral characteristics observed so far, and their possible explanation and significance to the discrimination problem. Figure 1-1 shows the average spectral energy distribution of the Øyer subarray beam formed on the P-wave from eight presumed explosions from central Asia and eight earthquakes from central Asia and southeastern Europe. Each individual spectrum was normalized to the total energy in the band from 0 to 3.0 Hz before averaging. The most striking contrasts in this comparison are the extended high frequency content and the well-developed minimum (centered at about 1.4 Hz) of the explosion average. It must be noted that the locations of the presumed explosions have a tighter spatial grouping than the earthquakes. Until the crustal structure beneath NORSAR is more fully understood, it cannot be said unequivocally that the observed spectral contrasts are due to source phenomena.

To date, a simple model has been considered to determine if the shape of the explosion spectra at NORSAR can be explained from elementary considerations. Figure 1-2 shows the result of a sequence of assumed processes including an idealized impulsive source, its prolongation in time, the near-source surface reflection, path attenuation, and seismometer response. At present, crustal effects are omitted.

Blake's[1] solution of the displacement spectrum due to a pressure impulse on the wall of a hollow sphere in an infinite elastic medium was generalized to include Q-type loss in the medium through the designation of complex velocities. Figure I-2(a) shows the relative log of the displacement spectrum plotted against frequency for radii of the hollow sphere ranging from 0.1 to 0.5 km at a distance of 10 km. This range in radii corresponds roughly to two orders of body wave magnitude (m_b). A reasonable model for the medium was assumed.

Figure 1-2(b) shows the effect of allowing the source pressure pulse to vary as $te^{-\eta t}$ where $\eta = 1.5 \sec^{-1}$. This value of η is consistent with other explosive source parameter studies (see Toksoz, et al.[2]).

The P-wave reflection (pP) at the earth's surface near the source is assumed to be of the form $Af(t - \tau)$, where $f(t)$ is the direct arrival, A is the surface reflection coefficient and τ is a time delay. Assuming A to be negative, the spectral effect of reflection is a multiplicative term of the form $[1 + A - 2A \cos \omega \tau]^{1/2}$ which introduces a modulation of the spectrum, specifically minima at frequencies (N/τ), $N = 1, 2, 3 \ldots$. Figure I-2(c) shows this effect for $\tau = 0.7$. At a distance of 38°, this delay would correspond to a depth/velocity ratio of 0.31, or a burial depth of 1.1 km, assuming an overburden velocity of 3.5 km/sec. Minima in the spectra of U.S. explosions recorded at LRSM stations have been attributed to this effect by Cohen.[3]

The overwhelming effect on the shape of the short-period seismic spectrum is that of attenuation, which at frequency f_o is assumed to be of the form $\exp[-\pi f_o t^*]$. Here $t^* = \sum_{i=1}^{n} t_i / Q_i$ where
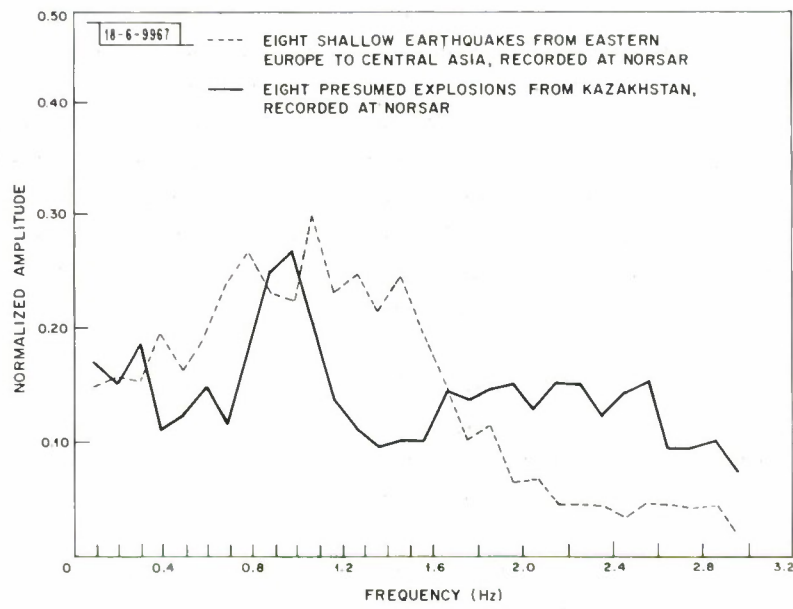
Fig. 1-1. Comparison of spectra of earthquakes and presumed explosions at NORSAR.
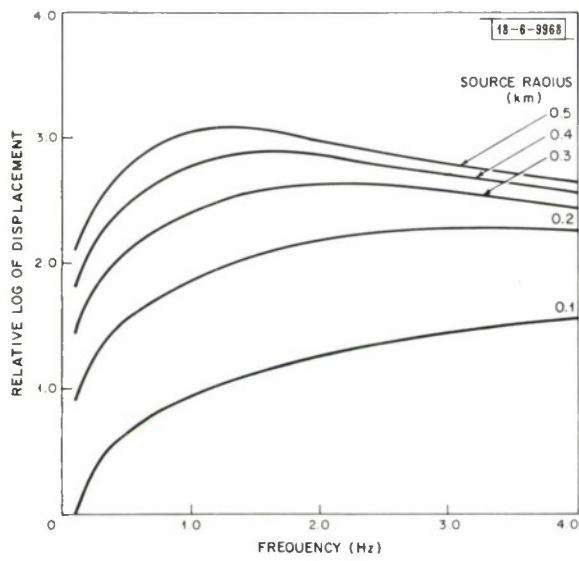
(a) Displacement response of infinite elastic medium due to pressure impulse on walls of hollow spherical cavities of various radii.
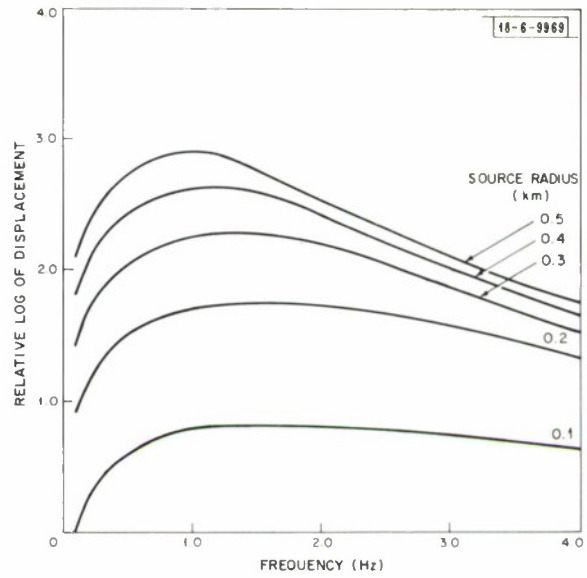
(b) Spectral effect of finite time duration of pressure pulse of form $te^{-\eta t}$ for $\eta = 1.5$.
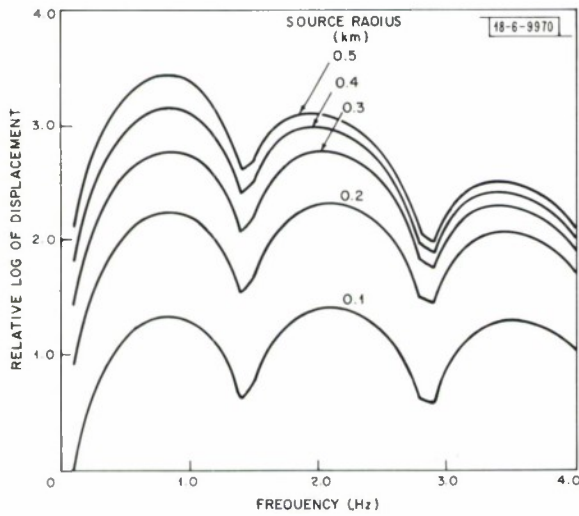
(c) Spectral effect of elastic reflection at free surface near source delayed 0.7 sec with respect to direct arrival.
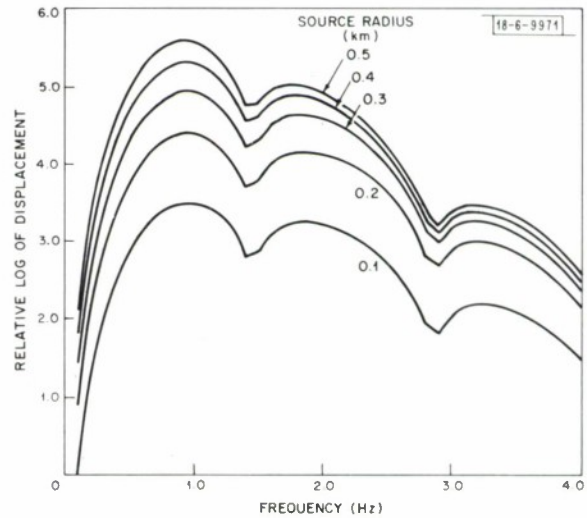
(d) Spectral effects of attenuation ($t^* = 0.6$) and instrument response.

Fig. I-2. Stepwise synthesis of theoretical explosion spectrum.
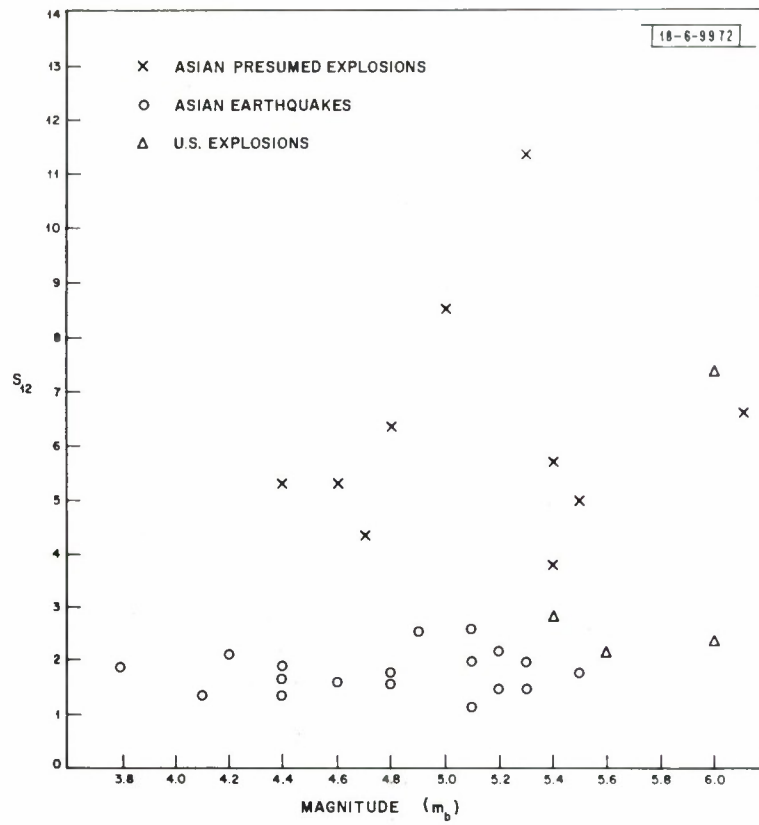
Fig. I-3.   NORSAR discrimination using spectral ratio S_{12}.

t_i is the travel time of a ray through n layers of a model earth, each with an assigned Q_i. Computations of t* were made by using the P-wave velocity model of Herrin, et al.,[4] and various Q-models. Values of t* at 40° computed for Teng's[5] Q-models, all of which have a low-Q (Q < 200) region in the upper mantle, ranged from 1.6 to 7.7. For the model considered here, a value of t* ≈ 0.6 is required in order to get significant energy in the 1.5- to 2.5-Hz band relative to the 0.5 to 1.5 band, as observed. At a distance of 40°, this value of t* is equivalent to a constant Q ≈ 600 in the upper mantle to a depth of 900 km. The geophysical implication is that there is a relatively high-Q region in the upper mantle under eastern Europe and western Asia.

After correcting for instrument response, Fig. I-2(d) shows the log of the amplitude spectra computed for t* = 0.6. The theoretical spectra of this figure show salient features of the average experimental spectra, i.e., a minimum at about 1.4 seconds, corresponding to a delay of 0.7 second, and significant energy to the right of this minimum in the 1.5- to 2.5-Hz band. If the mathematical model of the explosion spectra is at all accurate, the observed features of the central Asian explosion spectra may be genetic in origin and could be considered for discrimination purposes.

As a preliminary attempt, the spectral ratio

$$S_{12} = \frac{S_1 + 2 \cdot S_3}{S_2}$$

was formed, where S_i represents the sum of spectral components on the following bands:

i	Hz
1	0.63 to 1.06
2	1.22 to 1.65
3	1.88 to 2.31

The motivation here was to get a large value for explosions by exploiting the 1.4-Hz minimum and the extended high frequency content of the explosion spectra. The values of S_{12} were computed for 10 presumed Asian explosions and 18 shallow (h < 100 km) earthquakes with epicenters in central Asia and southeastern Europe and plotted against body wave magnitude in Fig. I-3. Clear separation of the Asian events was achieved. These initial results provided encouragement to compute S_{12} for four U.S. explosions recorded at NORSAR. Here only the event "Faultless" (in central Nevada rather than NTS) grouped with the Asian presumed explosions, while three NTS explosions grouped with the Asian earthquakes. The spectral minimum assumed due to burial occurred at generally lower frequencies (1.0 to 1.3 Hz) in the NTS spectra compared to the Asian explosions, indicating a lesser burial depth or higher overburden velocity for the latter. Additionally, the relative energy in the high frequency band S_3 of the U.S. explosions is less than that of Asian explosions recorded at NORSAR.

The above discussion indicates that observed differences in the P-wave spectra of Asian earthquakes and explosions may be due to source phenomena and if so these differences could provide a useful regional discriminant. Apparently the next step is to account for the spectral effects of the crustal structure under NORSAR.

J. Filson

B. CAUSES OF INTERSITE SPECTRAL DIFFERENCES

The lateral variations in the low-Q zone of the upper mantle is of immediate interest in nuclear test discrimination for two reasons. First, when choosing a site for a new seismic array, one seeks a location where short-period teleseisms are attenuated as little as possible by the low-Q zone of the upper mantle beneath the array. When modifying a short-period spectral discriminant for application at a new site, one must consider the difference in the Q of the upper mantle under the two sites.

A recent study[6] has provided a global map of the lateral variation of Q_β in the upper mantle. One can reasonably assume that the Q_α affecting short-period compressional waves has a similar lateral distribution. Q_β and Q_α are shear and compressional wave Q-values.

We are presently conducting a study to determine quantitatively the intersite differences in Q_α of the upper mantle. The three seismic arrays included in the study are the Norwegian Seismic Array (NORSAR), LASA, and TFSO. According to the map of Molnar and Oliver[6] and assuming that Q_α and Q_β are related approximately linearly, we expect a priori that the Q_α of the low-Q region under TFSO will be lowest, i.e., most inefficient transmission, and the Q_α under NORSAR the highest.

The method of analysis we are using is similar to that described by Teng.[5] We use a number of earthquakes recorded well at two sites. We compute the spectra of the beam output at each array for a 10-second time window. The ratio of each spectral component at the two sites is formed. Assuming that the source function $S(\Theta, \varphi, t)$ can be written

$$S(\Theta, \varphi, t) = S_t(t) \, S_s(\Theta, \varphi) \quad ,$$

the source time function is canceled by forming this ratio. After correcting for differences in the crustal response at each site and for instrumental differences, the logarithm of each spectral component is taken. The slope of this reduced spectral ratio is a measure of the differences in t* where

$$t^* = \pi \int_{ray} \frac{ds}{Q_\alpha \alpha} \quad .$$

The intersite difference $\Delta t^* = t_i^* - t_j^*$ has two contributions, one due to differences in distance between the source and each site, the other due to differences in the Q along each ray.

The effect of difference in source-receiver distance can be removed by relying on a worldwide Q_α distribution as given by Teng. More ideally, this effect can be removed by taking events equidistant between two sites. The remaining attenuation can then be attributed to differences in Q along the two ray paths. One would expect greater lateral homogeneity with increasing depth. Also, since the low Q of the upper mantle influences the total attenuation more than any other part of a ray path, the Q-value of this low-Q layer seems the most likely parameter to account for the intersite differences in attenuation. The low-Q layer of the upper mantle is usually traversed twice by a ray path, once at the source and once at the receiver. One must exercise care in determining whether the differences in attenuation of an event arriving at two sites is due to receiver or source path differences. To study the differences of the Q-layer at the receiver, the source region contribution must cancel when the ratio mentioned above is taken. Most ideally, one would select very deep events occurring near the lowest portion of the low-Q layer. However, events are not, in general, both very large and very deep.

6

Thirteen earthquakes recorded digitally at both LASA and NORSAR have been selected for study. They all have a high signal-to-noise ratio and occur approximately equidistant between sites. Unfortunately most of the events are shallow. Further events will be needed which are deep though not equidistant between LASA and NORSAR. Data recorded at TFSO and LASA are being collected.

Preliminary spectra computed on the data analysis console indicate that our initial supposition that events recorded at TFSO are most severely attenuated while those recorded at NORSAR are least severely attenuated is correct. The lateral variations of the low-Q zone in the source region seem to greatly affect the sensitivity of a given site to a particular region. For instance, if the ray path from an oceanic ridge event to a site lies perpendicular to the ridge, that site will be relatively more sensitive than a site whose ray path lies parallel to the ridge.

Quantitative estimates of the Q under each site are being sought using more precise calculations with data.

R. W. Ward (M.I.T. Earth
and Planetary Sciences Dept.)

C. CONTINENTAL APERTURE SEISMIC ARRAYS

The continental aperture seismic array computer program has been used to process data for an underground nuclear explosion and an earthquake. The purpose of the program is to determine the depth of an event by recognizing the arrival of the pP phase, making use of $P - pP$ differences in velocity, and to determine the P-wave source structure of the event by essentially steering many beams in the vicinity of the epicenter of the event. The data consist of the digitized and merged records from LASA and LRSM sites located in North America.

The program operates by assuming that the epicenter, but not the depth, of the event is known, as well as the P-wave arrival times at all the stations comprising the continental array. These times are computed from travel time tables, using the known station locations and the event epicenter. The P-waves at the various stations are brought into time alignment by an analyst. All beamforming operations are done on the aligned traces and the time delays used are computed from travel time tables, relative to the previously computed P-wave arrival times. This procedure is used in the hope that the need for using station corrections is eliminated. Amplitude weights are employed and are determined by using the calibration data for the stations, and by compensating for the different P-wave attenuation caused by the different distances of the stations to the epicenter.

The presence of the pP phase is determined by performing a beamforming operation over the network stations at successive times and with proper interstation delays corresponding to trial depths ranging from 10 to 200 km. The power of the beam output over the appropriate 1-second interval is computed as a function of the trial depth and the trial depth that corresponds to the peak of these powers is then taken to be the true depth.

The computed value of depth is used in the determination of the structure of the source P-phase and coda. A beamforming operation over successive 2-second intervals, starting with the P-arrival time, is performed. This results in a plot of power vs various latitudes and longitudes about the source hypocenter at the computed depth, with one contour plot for each 2-second interval. A theoretical network beam pattern is also computed and plotted in a similar manner to provide a basis for comparison with the experimental results.

7

18-6-9973

SITE

SVQB

PGBC

RKON

HNME

LAF1

LAF4

LAAO

LAF2

LAF3

KCMO

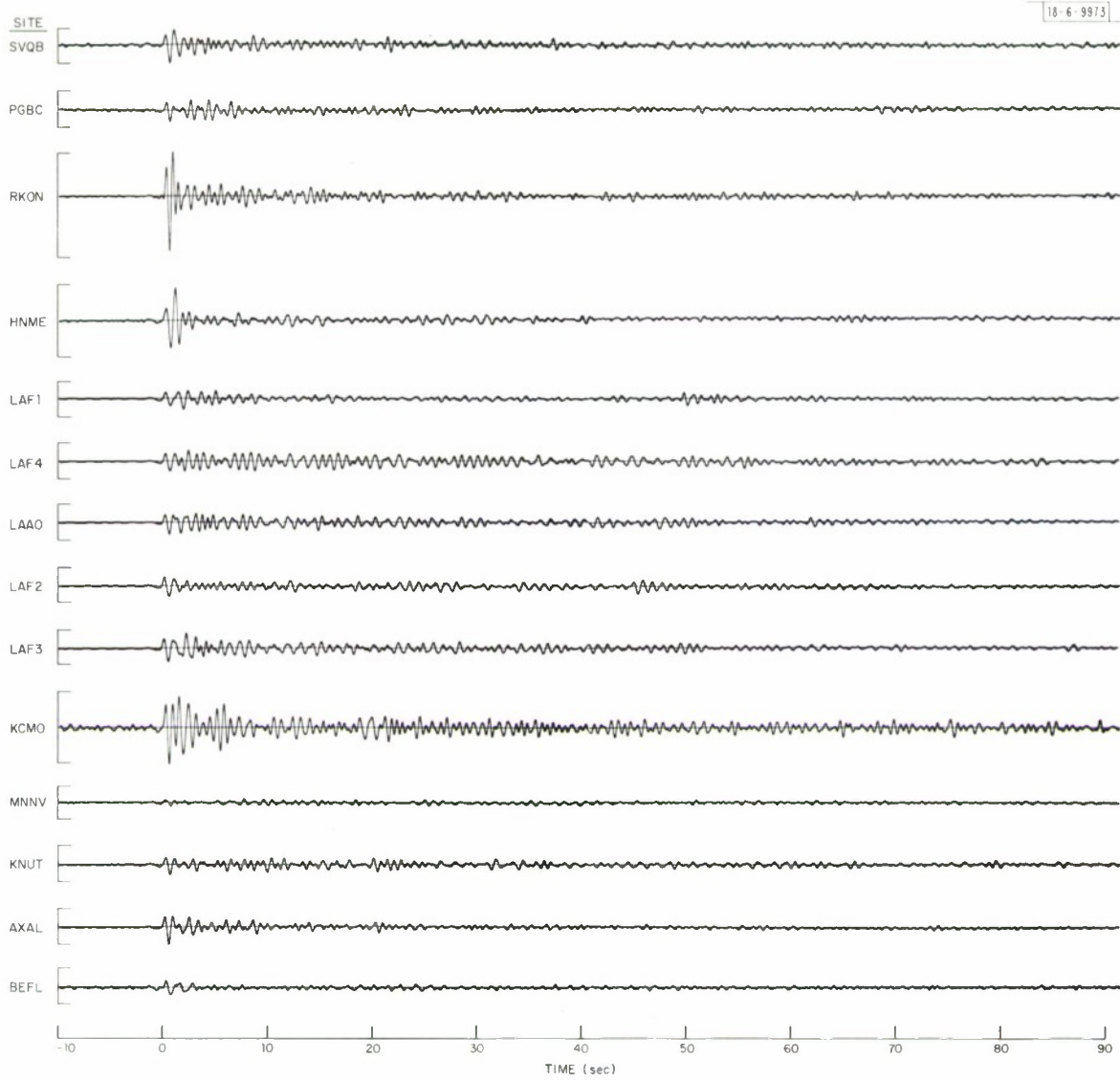MNNV

KNUT

AXAL

BEFL

TIME (sec)

Fig. 1-4. Wavefarms far 27 Octaber 1966, Navaya Zemlya event.

The program has been used to process the 27 October 1966 Novaya Zemlya explosion, m_b = 6.3 (USCGS). The data from the various stations used is shown in Fig. I-4. The stations are distributed over an aperture of about 4300 km and vary in distance from the epicenter from 46° to 74°. For this event, the determination of depth by the program is not meaningful and the depth is assumed to be 0 km.

The waveforms of Fig. I-4 show striking differences in waveshape for this event as viewed across the network. For example, the waveforms observed at RKON, HNME are very simple while those at LASA, i.e., the subarray straight sums from LAAO, LAF1, LAF2, LAF3, LAF4, are extremely complex. These data show that some caution must be exercised in employing the complexity criterion for discrimination.

The differences in waveshape at each station are believed to be caused by the complex crustal structure at each site. An attempt was made to design equalization filters which would compensate for the distortion in waveshape introduced by the receiver crustal structure. However, these attempts produced results which were believed to be largely unsuccessful. Thus, it appears to be impractical, at the present time, to remove the effects introduced by local crustal structure.

Fortunately, it appears that in some cases the severe distortion introduced by the local crust may not prevent the determination of source structure by means of beamforming. The results of such a computation for the same Novaya Zemlya event are shown in Figs. I-5(a-e). The beam output power is displayed as contours, in decibels relative to the peak output beam power, ranging from 0 to 10 dB in increments of 1 dB. The X in each figure represents the location of the epicenter provided by USCGS, and the O corresponds to the location from which the peak power output is provided by the beamforming process. In Fig. I-5(a) the O and X coincide, indicating that during the first two seconds after the origin time the peak power is coming from the epicenter. In Figs. I-5(b-e) we see a migration of the location providing the peak power. These locations are indicated in Fig. I-5(c) along with a map of the Novaya Zemlya region.

The migration of the location of the zeros in Figs. I-5(a-e) is compatible with conditions imposed by known seismic compressional wave velocity in the crust. That is, the location of the zeros appears to shift by about 20 km between successive 2-second frames and this is compatible with a compressional wave whose velocity is about 6 km/sec in the crust which is traveling toward the network. This wave may trigger a series of events whose epicenters are indicated in Fig. I-6. The peak power in successive frames of Fig. I-5 measured with respect to the first frame is 0, −1.7, −4.3, −4.1, and −4.8 dB. This relatively slow decrease of power level seems to eliminate the possibility that scattering of the compressional wave may be taking place.

It is not yet possible to state that the migration of the locations of the zeros in Fig. I-5 is meaningful. In order to check whether the migration is real, a test was made by observing it when two disjoint sets of stations were employed in the beamforming process. For both of these disjoint sets, the migrations were in reasonable agreement with the results shown in Fig. I-5. In addition, there is a good agreement between Fig. I-5(a) and the computed theoretical network beam pattern. However, there is one disturbing aspect to the data indicated in Fig. I-5(c): in the upper-right-hand corner of this figure, there is a 1-dB contour. The emergence of such a contour is difficult to explain, since its distance from the epicenter is not compatible with known seismic velocities. This contour may be caused by the distortions introduced by local crustal structure, as mentioned previously, and these distortions may, in some cases, be so severe as to prevent the determination of source structure.
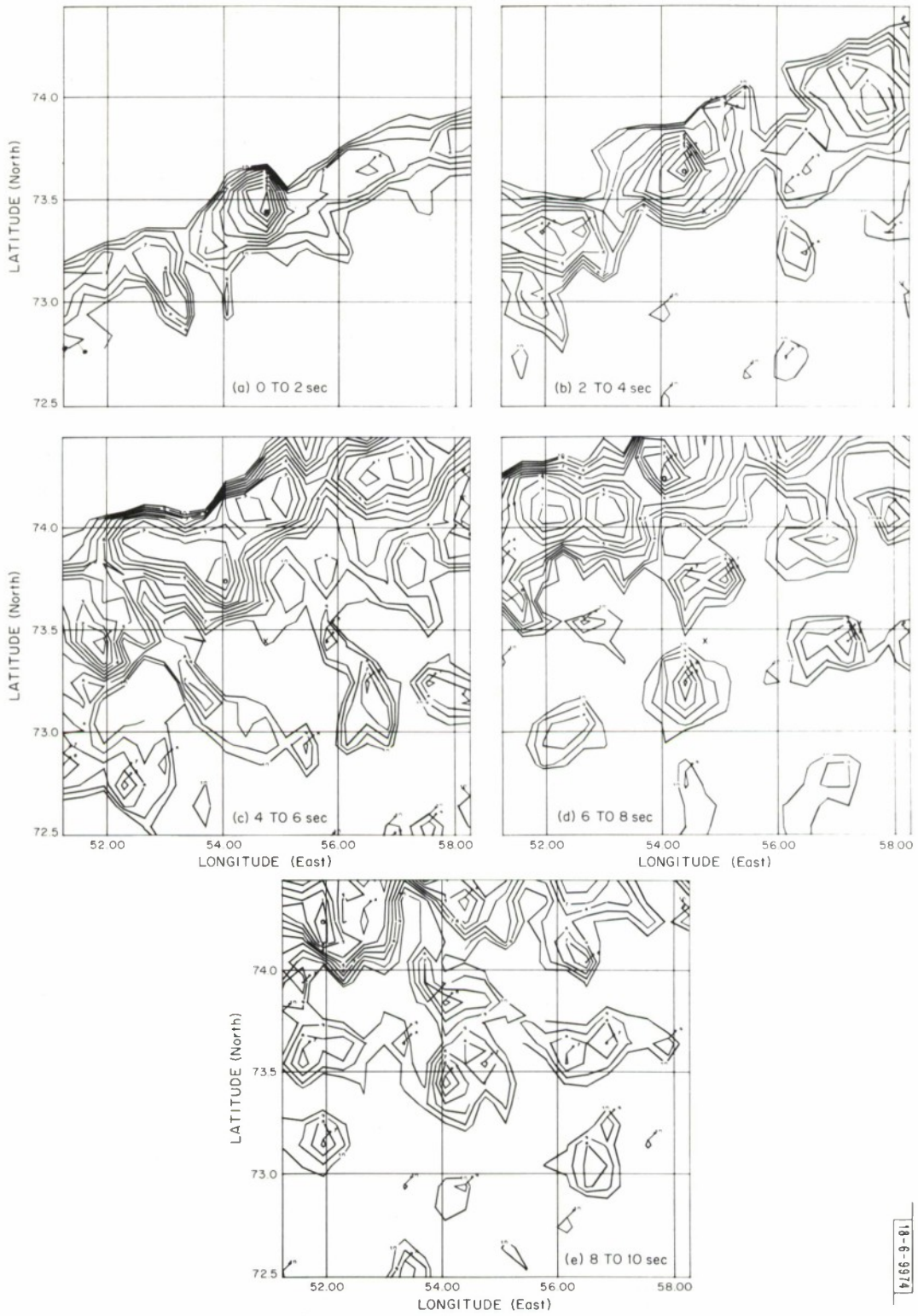
9

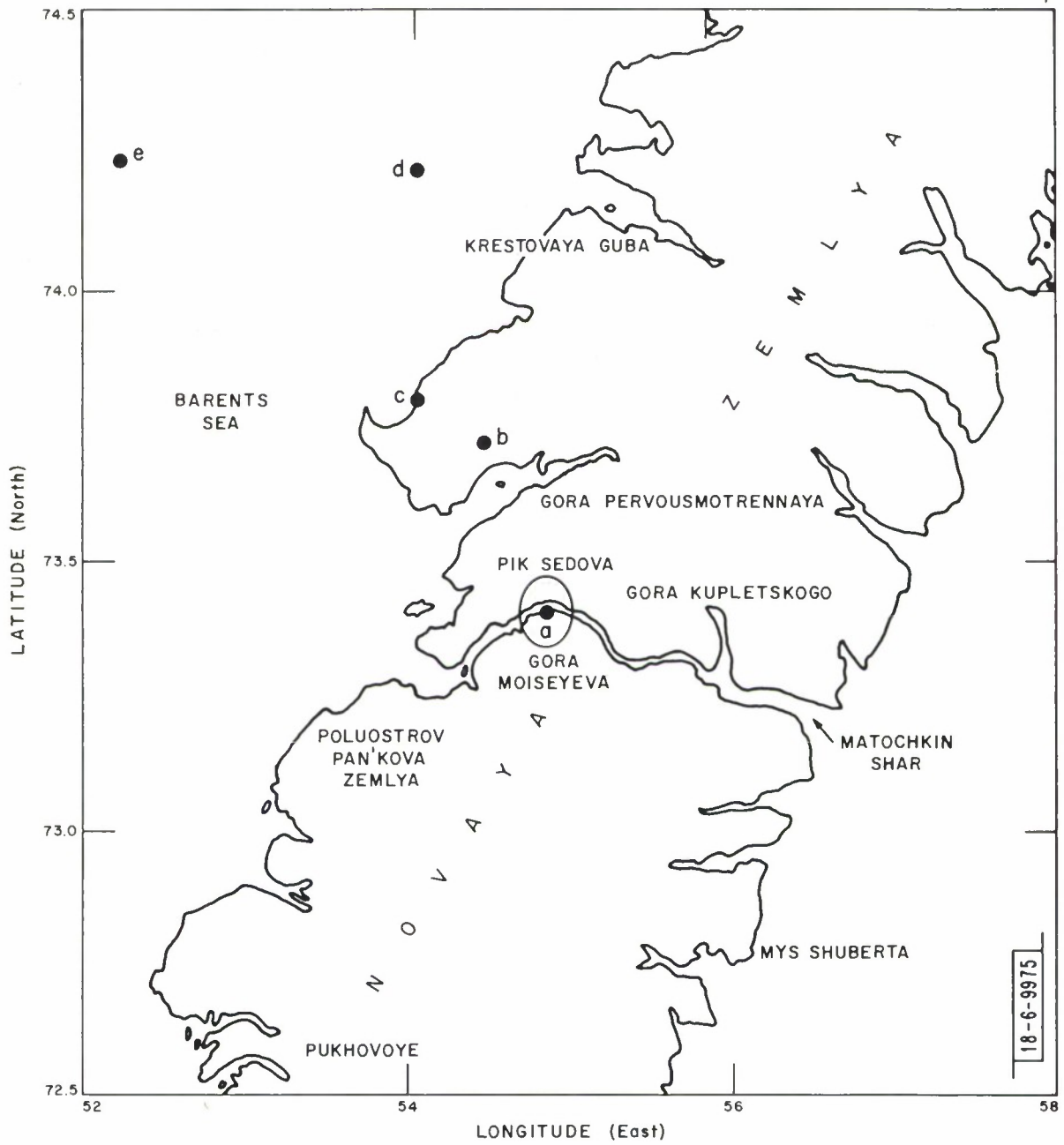Fig. I-5. P-wave source structure result for 27 October 1966, Navaya Zemlya event.

Fig. I-6. Migrotion of locotion of peok power for 27 October 1966, Novoyo Zemlya event.

The program has also been used to process the 9 February 1967 Colombia event. The USCGS listed the m_b for this event at 6.3 and restrained the depth to 58 km on the basis of observation of pP at four stations. However, the distortions introduced by local crustal structure for this event were so severe that no meaningful continental array results were obtained in either the pP determination or the source structure computation. At present, the data from seven more events are being digitized and merged so that the program may be tried on a variety of events.

<div align="right">J. Capon</div>

D. SURFACE WAVE ARRIVAL TIME PREDICTION

Rayleigh waves recorded at LASA with periods of about 20 seconds can be used to estimate surface wave magnitudes. Used in conjunction with body wave magnitudes, these can provide discrimination via the $M_s - m_b$ criterion.[7] The efficacy of the $M_s - m_b$ method depends to some extent, especially when there is a possibility of waves from interfering events, upon the reliability with which the arrival time of such waves can be predicted. This question has been examined using data from a large population experiment which has previously been conducted.[7]

Surface wave trains for nine presumed explosions and 31 earthquakes, all of which had clear Rayleigh phases recorded at LASA, were examined. The arrival time of 20-second waves from each event was picked by an analyst, using a beam of vertical instruments steered to 3.7 km/sec. In addition, the time of the peak of a chirp filter designed to introduce no delay at 20 seconds was recorded. By using the distance and the origin times given by the USCGS, a group velocity for 20-second waves was computed for each of the 40 events. The events have been broken into three groups and the results summarized in Table I.

TABLE I		
SURFACE WAVE GROUP VELOCITIES		
CONTINENTAL PATHS		
	Chirp Filter	Analyst	Central Asian
High	2.99	3.13	Earthquakes & presumed
Average	2.94	3.00	explosions
Low	2.90	2.96	14 events
PARTLY OCEANIC PATHS		
Pacific Ocean		
High	3.29	3.34	Kuriles Islands
Average	3.15	3.17	Earthquakes
Low	2.97	3.01	16 events
North Atlantic Ocean		
High	3.11	3.16	Southwestern USSR
Average	3.02	3.07	Border lands
Low	2.89	3.01	Earthquakes
			10 events

The scatter of group velocities for the continental paths corresponds to a scatter of arrival times of roughly ±1 minute, whereas the corresponding figures for the Pacific and North Atlantic partly oceanic paths are about ±2-1/2 and ±2 minutes, respectively. The variations resulting from the use of group velocity from one path for predicting arrival time for another path is in the range of 1 to 2-1/2 minutes. Thus, regionalization of group velocity values would be helpful; the predicted arrival times of 20-second waves should then be in error by no more than several minutes with the amount being a function of epicenter. Events having partly or completely oceanic paths may have more scatter because the slope of the group velocity curve at 20 seconds can be quite steep. Small changes in path or period can have larger effects for oceanic than for continental paths.

E. Rygg
University of Bergen

E.   DECISION PROBABILITIES FOR LONG- AND SHORT-PERIOD DISCRIMINANTS

A LASA large-population discrimination experiment and some of the implications of the data obtained from the experiment were described in our previous Semiannual Technical Summary Report.[7] Since that time, a more complete description[8] has been published giving results in considerably more detail. Since the appearance of that report, the data have been analyzed further in an attempt to estimate several important probabilities. The principal results of this analysis will be presented in a Technical Note and are summarized below.

Both the $M_s - m_b$ criterion, a long-period discriminant, and the modified spectral ratio (MSR), a short-period discriminant, were described earlier.[7] Most studies of such discriminants have emphasized their value under the implied assumption that all measurements required by the decision rule could be obtained with a sufficient signal-to-noise ratio to be valid. However, it is also important to determine the probability that the noise will make the appropriate measurement invalid so that a particular discriminant cannot be applied. For example, assuming that an m_b measurement has been obtained at LASA, what is the probability that the MSR or the $M_s - m_b$ criterion can be applied using LASA data?[8] The probability will depend upon the m_b value and whether the event is an explosion or an earthquake. It should be noted that we are not discussing the probability of correct identification, but the magnitude-dependent probability that the discriminant will give a decision. However, since both $M_s - m_b$ and the MSR have a high probability of correct identification when they do generate a decision, it is clear that the functions we are considering are only slightly larger than the probabilities of correct identification at any m_b level.

Figures I-7 and I-8 display the principal results. If an event is an earthquake of magnitude m_b it is clear from Fig. I-7 that the MSR has a slightly higher probability of yielding a decision than does $M_s - m_b$. However, the ability of the MSR to operate at a lower magnitude than $M_s - m_b$ is only very slight for earthquakes. Roughly, the probabilities in both cases drop from 1.0 to 0.0 as m_b goes from 5.0 to 4.0. The situation is considerably changed in the case of explosions (Fig. I-8). In this case, the probability for the MSR is about the same as it is for earthquakes. However, for $M_s - m_b$ the probability of obtaining a decision drops from 1.0 to 0.0 roughly as m_b goes from 5.2 to 4.5. Thus MSR can be of significant value especially in the 4.0 to 5.0 range, since it tends to yield a decision for a significantly higher percentage of the explosions than does $M_s - m_b$.
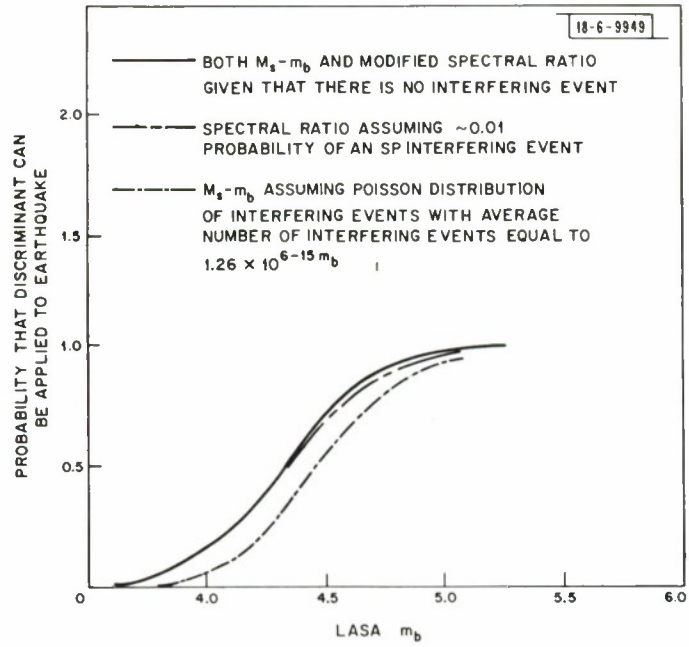
R. T. Lacoss

13

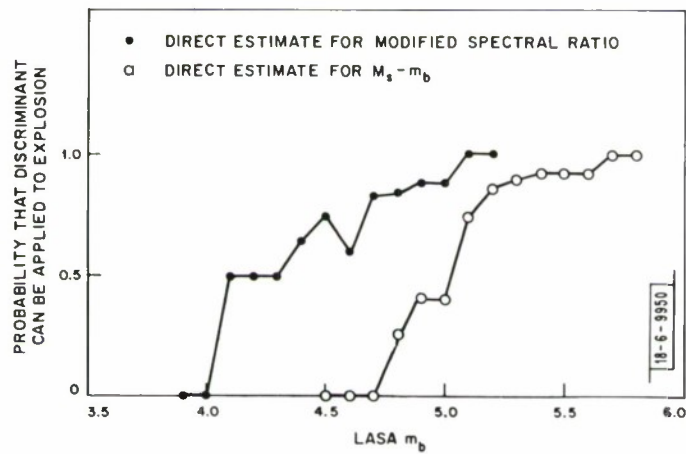Fig. I-7. Probability that LASA seismic discriminants can be applied to teleseismic earthquakes.

Fig. I-8. Probability that LASA seismic discriminants can be applied to teleseismic underground explosions.

REFERENCES

1. F. G. Blake, "Spherical Wave Propagation in Solid Media," J. Acoust. Soc. Am. 24, 211-215 (January 1952).

2. M. N. Toksoz, Ben Menahem A. and D. G. Harkrider, "Determination of Source Parameters of Explosions and Earthquakes by Amplitude Equalization of Seismic Surface Waves. 1. Underground Nuclear Explosions," J. Geophys. Res. 69, 4355-4366 (October 1964).

3. T. J. Cohen, "Determination of Source Depth by Spectral, Pseudo-autocovariance, and Cepstral Analysis," Teledyne, Inc., SDL Report No. 229, 24 January 1969.

4. E. Herrin (Chairman), and the 1968 Seismological Tables Working Group, "P Wave Velocity Distribution in the Mantle," Bull. Seismol. Soc. Am. 58, 1223-1225 (August 1968).

5. T. Teng, "Attenuation of Body Waves and the Q Structure of the Mantle," J. Geophys. Res. 73, 2195-2208 (March 1968).

6. P. Molnar and J. Oliver, J. Geophys. Res. 74, 2648-2682 (15 May 1969).

7. Semiannual Technical Summary Report to the Advanced Research Projects Agency on Seismic Discrimination, Lincoln Laboratory, M. I. T. (31 December 1968), Sec. 1, DDC 682297.

8. R. T. Lacoss, "A Large-Population LASA Discrimination Experiment," Technical Note 1969-24, Lincoln Laboratory, M. 1. T. (8 April 1969), DDC 687478.

II. MISCELLANEOUS PROJECTS

A.   STATISTICAL ESTIMATION OF SEISMICITY AND DETECTION PROBABILITY

Suppose that we have a catalogue of earthquakes, i.e., a list of events, giving magnitude and hypocentral parameters, which occurred in a given region, during a given time interval, as determined by a fixed seismic network. Suppose further, that it is desired to obtain from these data estimates of the seismicity parameters of the region and also some measure of the detection performance of the seismic monitoring system. By making simple assumptions regarding the statistical character of both the earthquake-occurrence process and the system detection process, we have formulated this question as a statistical parameter estimation problem and obtained solutions for the estimates.

Specifically, we assume that the occurrence of earthquakes (irrespective of hypocenter) is a Poisson process, and that the mean number of events, $N(m_b)$, having body wave magnitude at least m_b, is given by

$$\log N(m_b) = a - bm_b \quad ,$$

where a and b are parameters to be estimated. The detection system (seismic network) is characterized by a probability of detection, $P(m_b)$, of an event of magnitude m_b, in the form of an error function

$$P(m_b) = (2\pi\sigma^2)^{-1/2} \int_{-\infty}^{m_b} \exp\left[-\frac{(m-\mu)^2}{2\sigma^2}\right] dm \quad ,$$

where μ and σ are parameters to be estimated. A likelihood function can now be written and expressions for the maximum likelihood estimates of a, b, μ and σ obtained.

We have obtained explicit formulas for the $\hat{a}$ and $\hat{b}$, the estimates of a and b, given μ and σ. They agree with known results[1,2] when it is assumed that only events larger than some $m_o = \mu$ are used, and that the system has detected all such events (that is, $\sigma = 0$, $\mu = m_o$). In the general case, the remaining parameters μ and σ are obtained numerically by minimizing the likelihood function, assuming that $a = \hat{a}$ and $b = \hat{b}$. This minimization is accomplished by computing the likelihood function on a grid of values of σ and μ and contouring the result. Figure II-1 shows the outcome of an experiment which used the first 2000 events reported by the USCGS in 1968. The likelihood function and $\hat{b}$-function have both been contoured on the μ, σ plane. The maximum of the likelihood function is obtained at $\mu = 5.1$, $\sigma = 0.415$, which corresponds to b = 1.725.

Given μ, σ, and b, it is possible to compute the expected percentage of events which will be recorded at or above any magnitude level. Figure II-2 shows the experimental data used in the above experiment and the theoretical curve corresponding to the μ, σ, and b values which were obtained. The good agreement between the curves is one indication of the relevance of our statistical model and the applicability of the maximum-likelihood method to the total problem of estimating seismicity and detection capabilities.

<div align="right">
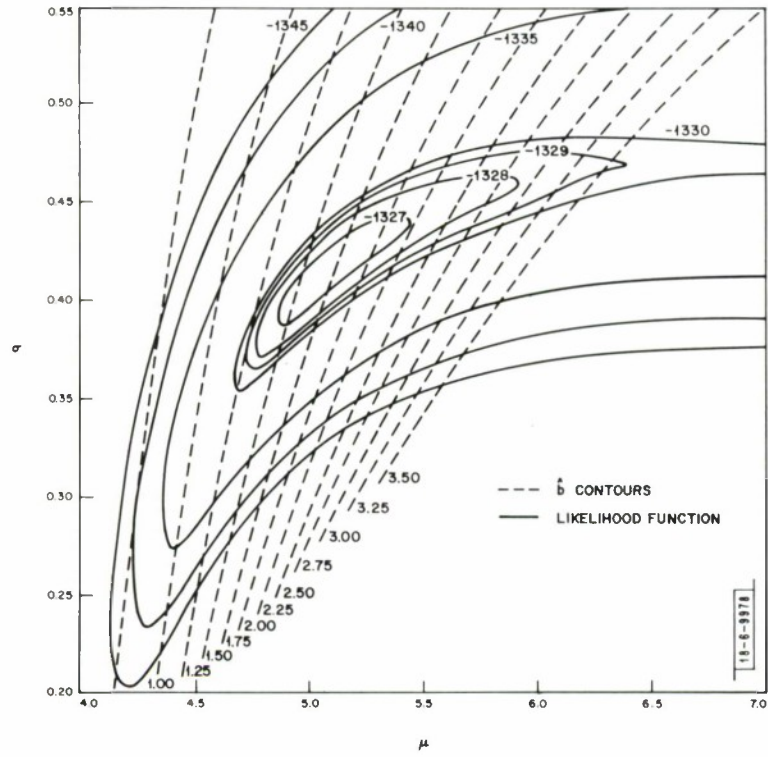
E. J. Kelly
R. T. Lacoss

</div>

Fig. II-1. Likelihood function ond estimated seismicity porometer os function af detection network porometers (based on 2000 USCGS events).
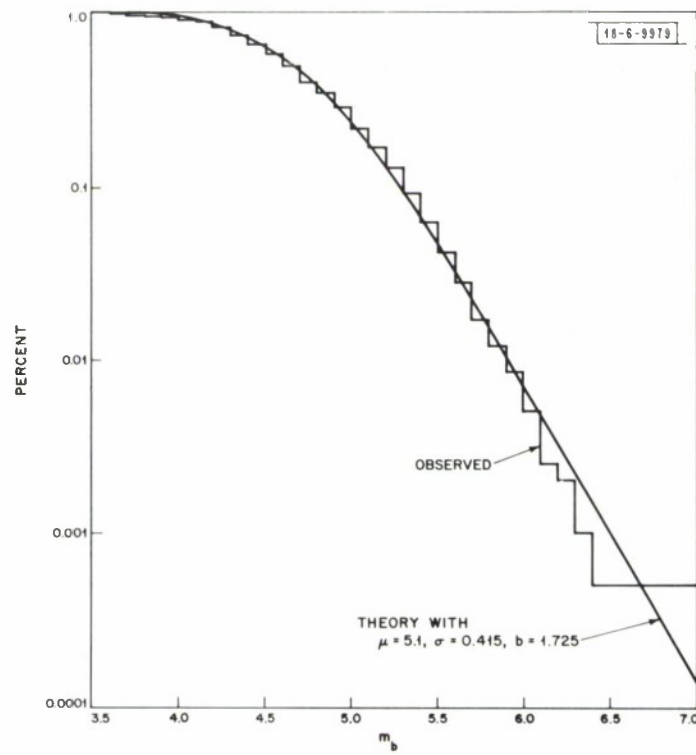
Fig. II-2. Cumulative histogram of 2000 USCGS events and theoretical curve obtained from maximum-likelihood estimate of seismicity and network performance.

B. COMPUTER-GENERATED SEISMICITY MOVIES

The use of computer-generated movies to study the spatial and temporal variation of epicenters has been shown to be an interesting and novel approach to the study of worldwide or regional seismic activity.[3] A computer generated movie will consist of several thousand plots or frames each containing a map or outline of the land masses and several points indicating the locations of epicenters that occurred during some finite time interval. The magnitude of each event can be used to determine the number of additional frames on which the epicenter will appear and the brightness of the point that represents the epicenter. Thus large events will appear visible for a longer period of time and with greater brightness than will a small magnitude event. The final film will contain the seismic activity for several months or years which one can view within a matter of a few minutes.

A computer-generated movie of the Kurile Island earthquake swarm of 1963 was produced. The film covers the months of October and November during which most of the seismic activity in this swarm occurred. Each frame on the film contains all the events that occurred during one hour. Thus 24 frames equal one day and, when projected, one day could be viewed in one second of real time. This film covered 61 days, contained over 500 events and could be viewed in little over one minute.

The film revealed some very interesting aspects of this earthquake swarm. The one most obvious fact is that the epicenters migrated seaward from the island arc at a rate of approximately 100 km/hour. This seaward migration occurred in several cycles during most of the aftershock activity. Other obvious facts include the lack of activity in the Sea of Okhotsk and the concentration of seismic activity to only a few regions within the Kurile Island chain.

Several other movies are being produced to study the activity during the 1964 Alaskan earthquake, the 1964 Rat Island swarm, the 1968 Hokkaido swarm and the 1968 Easter Island swarm. It is hoped that motional trends can be recognized and some quantitative value can be assigned to each of these trends.

<div align="right">R. M. Sheppard</div>

C. LASER INTERFEROMETER MEASUREMENTS OF ATMOSPHERE

The demonstration of the feasibility of a 6328-Å laser interferometer through an atmospheric path of 7 km has been completed. The techniques can presumably be extended to a system operating at several optical wavelengths to correct for atmospheric refractive index and turbulence effects to obtain a true measure of earth strain buildup. The SATS dated 31 December 1967 carries a quite complete description of the method. Also included in that report were experimental results with a single laser over a path length of 1.5 km. Since that time, the interferometer system has been refined and the path length extended to 7 kms. For system details, the reader is referred to the earlier report.

The interferometer constructed to date is still a single laser wavelength system, and does not, therefore, measure earth movement independently of the atmosphere. The experimental results to date are primarily directed to establishing the degree to which the atmosphere follows theory, and the extent to which the optical phase stability conforms to values previously anticipated.[4-6] The results have been submitted as a journal article and a brief summary follows.

Three different properties of atmospheric propagation over 7 km were measured; slow phase drift, rapid phase fluctuations, and amplitude statistics. The last parameter, although of less direct concern to us, is of interest to atmospheric science, since it turns out to be the most sensitive to the precise atmospheric model. These laser measurements, by virtue of using coherent optical detection, provide a dynamic range of up to 5000:1 in intensity, or about two orders of magnitude over previous measurements. At the extremes of this range, the intensity statistics were found to depart severely from the commonly accepted log-normal distribution and also from the more recently proposed Rayleigh and Rice-Nakagami distributions. The standard deviation of the logarithm of the amplitude is a single parameter that describes the depth of the amplitude fluctuation. This parameter reaches a limiting value of 0.85, in accord with recent modifications of the mathematical theory of the atmosphere.[7]

Figure II-3 shows a typical plot of phase changes measured over a 4-second time interval, along with the corresponding amplitude functations. (A plot of intensity would show even more severe fluctuations, since the intensity is the square of the amplitude.) Of equal interest is the spectrum of the more rapid fluctuations in amplitude and phase, not discernible on the time scale of the above plot. The upper limit to the frequency spread of a laser beam propagating through a 7-km one-way (14-km round trip) path appears to be 300 Hz. This figure is valid as an upper limit, even though a large part of this spectral spread is contributed through the laser's sensitivity to mechanical vibration (a factor that would be greatly reduced were the laser from a seismic vault). This figure is quite close to the theoretical value expected for daytime conditions over such a path length and is well within the range of the fringe-crossing rate that can be handled by a strain-measuring interferometer system.

E. Gehrels

D. DATA PROCESSING FACILITIES

During the past six months, the offices and data processing equipment have been moved from Lexington to our new space at 42 Carlton Street, Cambridge, adjacent to the M.I.T. campus. One of the PDP-7s that was at the LASA data center in Billings, Montana, has also been moved to Cambridge and modified by the addition of extra equipment so that it will be identical with the existing machine.

A block diagram of the complete computer hardware is shown in Fig. II-4. All this equipment is operating, except for the following:

(1) The Beta hard copy printer has not been delivered.

(2) The 40.8 kilobaud data link, modems and associated equipment to interface to computer 2 have not been delivered.

(3) The shaft encoder, multiplexer and A/D converter, and knob box for computer 2 have not yet been built.

These three items should be completed shortly.

In addition, a modification of the DEC 340 display system has been designed by Lincoln Laboratory to decrease the time required to display a point from 35 to about 10 μsec.

A new software system for the PDP-7 has been designed and is shown in Fig. II-5. It consists of a permanently resident LOAD AND GO program that loads programs which are called
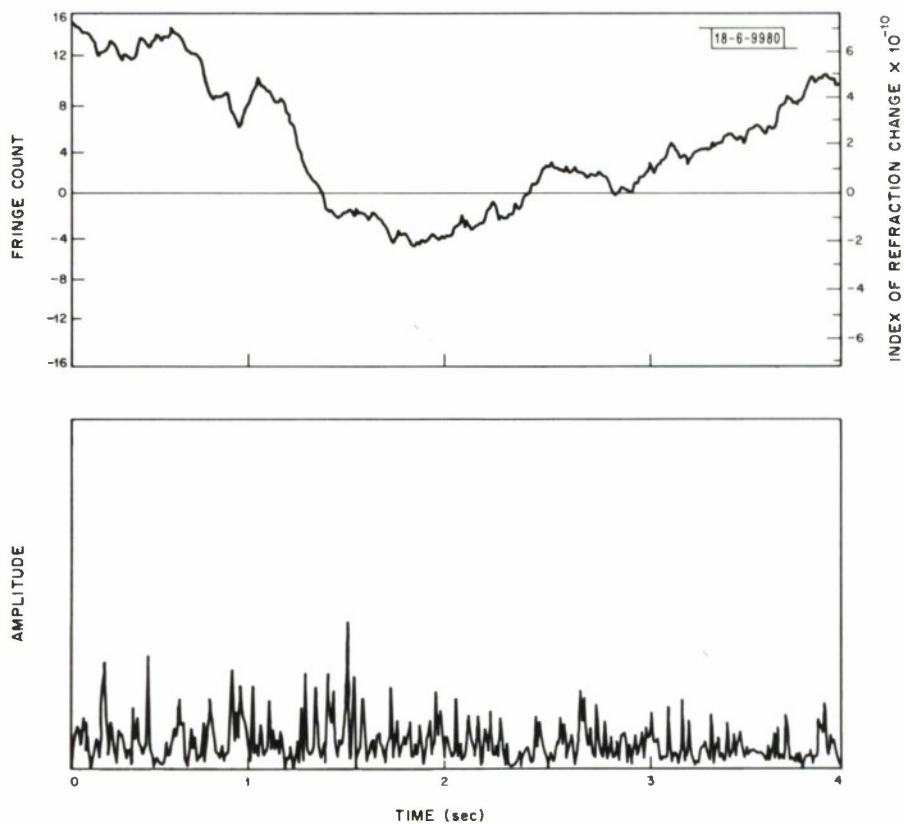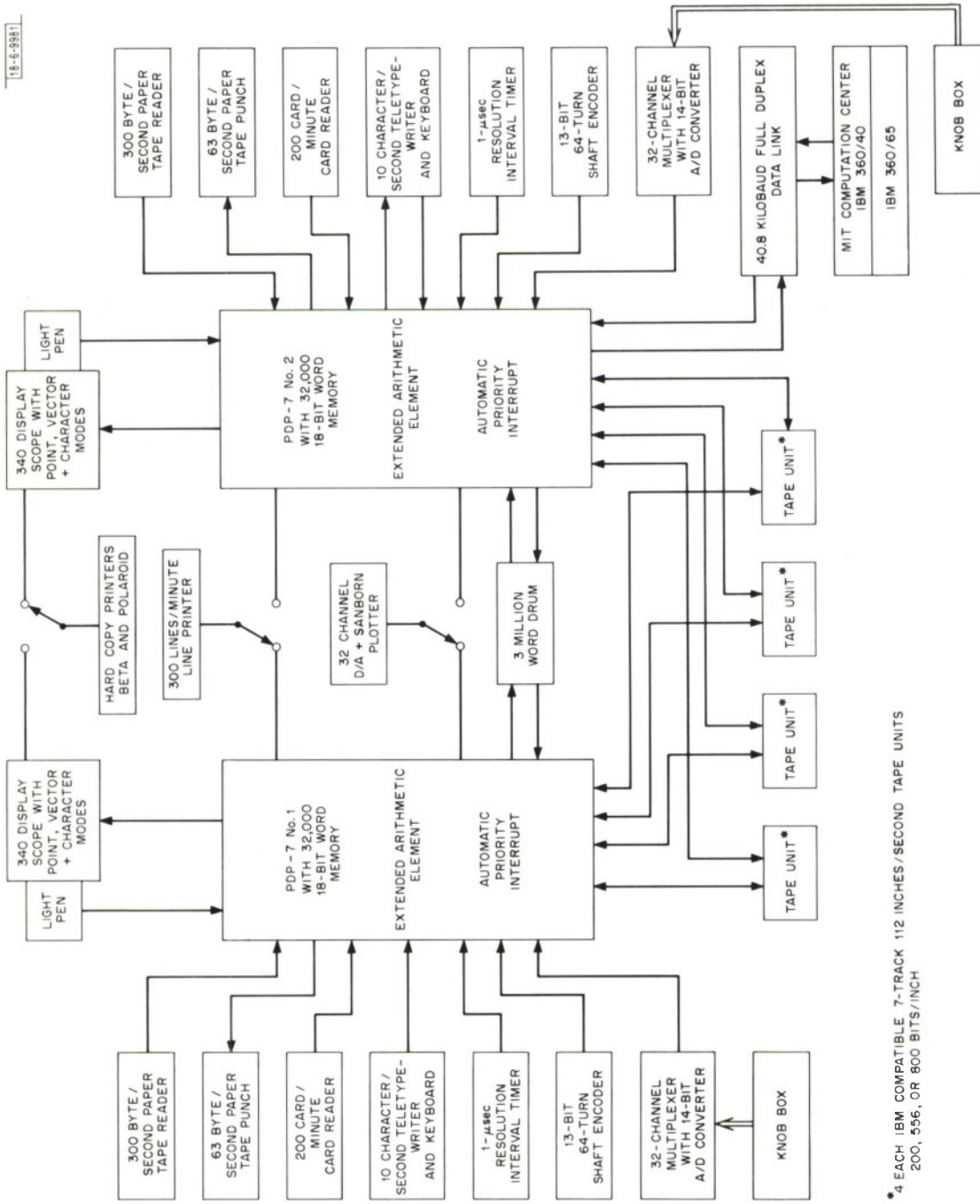
Fig. II-3. Atmaspheric phase and amplitude fluctuatians far 7-km interferameter path (29 July 1968, 1933 EDT).

18-6-9981

Fig. II-4. Cambridge computer center hardware.

* 4 EACH IBM COMPATIBLE 7-TRACK 112 INCHES/SECOND TAPE UNITS
200, 556, OR 800 BITS/INCH

300 BYTE/SECOND PAPER TAPE READER

63 BYTE/SECOND PAPER TAPE PUNCH

200 CARD/MINUTE CARD READER

10 CHARACTER/SECOND TELETYPE-WRITER AND KEYBOARD

1-μsec RESOLUTION INTERVAL TIMER

13-BIT 64-TURN SHAFT ENCODER

32-CHANNEL MULTIPLEXER WITH 14-BIT A/D CONVERTER

40.8 KILOBAUD FULL DUPLEX DATA LINK

MIT COMPUTATION CENTER IBM 360/40

IBM 360/65

KNOB BOX

LIGHT PEN

340 DISPLAY SCOPE WITH POINT, VECTOR + CHARACTER MODES

PDP-7 No.2 WITH 32,000 18-BIT WORD MEMORY

EXTENDED ARITHMETIC ELEMENT

AUTOMATIC PRIORITY INTERRUPT

HARD COPY PRINTERS BETA AND POLAROID

300 LINES/MINUTE LINE PRINTER

32 CHANNEL D/A + SANBORN PLOTTER

3 MILLION WORD DRUM

TAPE UNIT*

340 DISPLAY SCOPE WITH POINT, VECTOR + CHARACTER MODES

PDP-7 No.1 WITH 32,000 18-BIT WORD MEMORY

EXTENDED ARITHMETIC ELEMENT

AUTOMATIC PRIORITY INTERRUPT

LIGHT PEN

300 BYTE/SECOND PAPER TAPE READER

63 BYTE/SECOND PAPER TAPE PUNCH

200 CARD/MINUTE CARD READER

10 CHARACTER/SECOND TELETYPE-WRITER AND KEYBOARD

1-μsec RESOLUTION INTERVAL TIMER

13-BIT 64-TURN SHAFT ENCODER

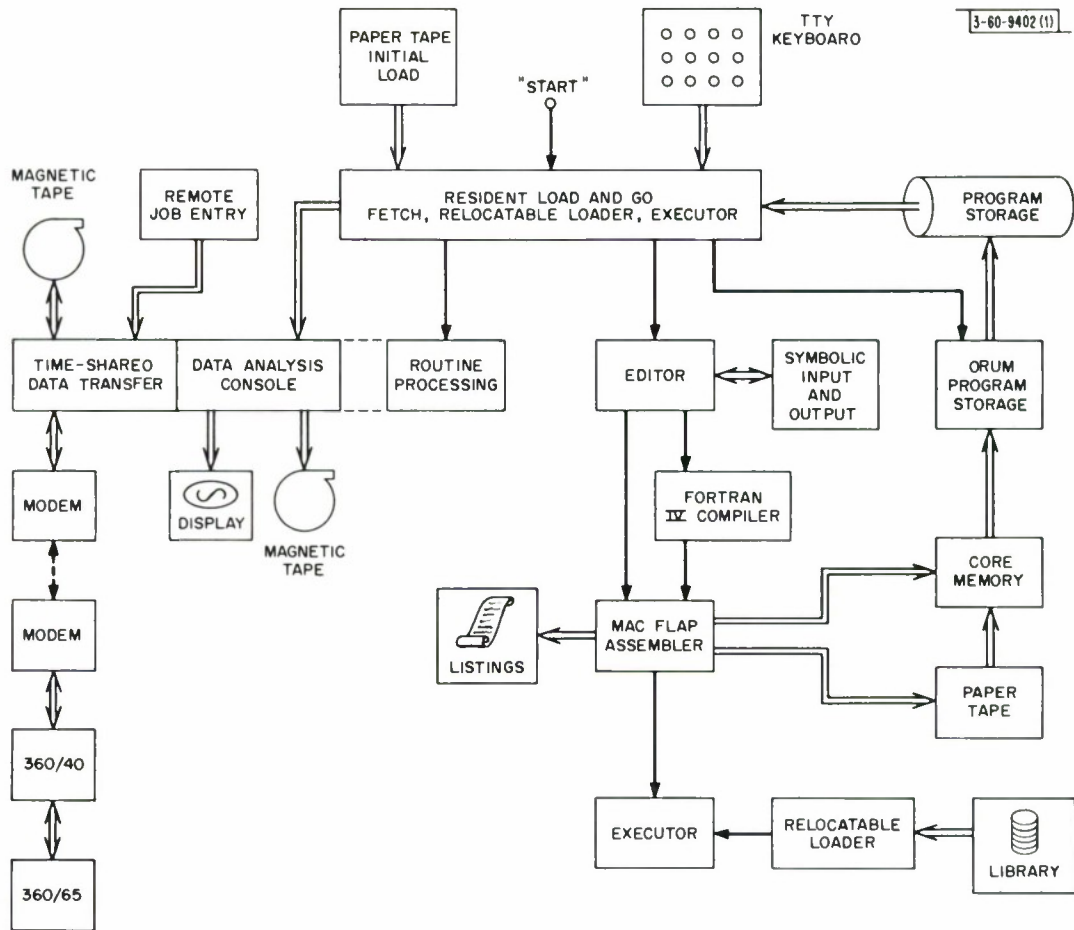32-CHANNEL MULTIPLEXER WITH 14-BIT A/D CONVERTER

KNOB BOX

23

Fig. II-5. PDP-7 software.

by the TTY keyboard.   All these other programs are stored on the 3×10^6 word drum and are loaded into the core memory by means of a relocatable loader.   When the new program is loaded, control is transferred to it.   Four types of programs are shown in the figure that can be loaded from this resident LOAD AND GO.

The first is called Routine Processing.   This is the collection of all our routine processing programs, e.g., magnetic tape plotting, duplication, checking and dumping, special system programs, etc.

The second is the new Lincoln Data Analysis Console.   The basic ideas of this system have been described in Lincoln Laboratory Technical Note 1968-14; however, the new console will have the added task of time sharing a remote IBM 360/40 to our magnetic tape drives and card reader.   This is to allow for remote job entries and input-output of large data bases (e.g., a reel or two of magnetic tape) to the IBM 360/65 machine at the M.I.T. Computation Center.   The 360/40 queues the job on a disk until the input process is complete and, when read, transfers the job for execution by the 360/65.   The output is handled in the reverse way.   When the system is complete, the "console" programs will be linked to the console executive routine in the same way that routine processing programs are linked to the resident LOAD AND GO program.   Thus any thoroughly debugged and frequently used program which conforms to the console conventions can be added to the "console" by simply adding it to the catalogue of routines available to the console executive.

The third is a symbolic test editor with a Fortran IV compiler and the Macflap assembler. The input can be on punched cards (IBM 029 code) or magnetic tape.   The source cards can be read into the scratch area of the drum and edited by the TTY keyboard or cards.   The editing is done on the Fortran statement numbers or the Macflap symbolic names (i.e., the characters punched in columns 1-6).   The editing commands are: Change, Move, Insert, Delete, Append, List, File, Save on Mag Tape (for future input), Assemble and Fortran.   The assemble command is used if the source is PDP-7 machine language in Macflap format and has been filed on the drum.   The Assembler, which is a relocatable subroutine of the Editor, takes the source from the drum and stores the binary version in an upper bank of the core memory and outputs, under ACC switch control, a listing and/or a punched binary paper tape.   The editing command Execute will load the program into the lower bank and transfer control to the starting location. The Fortran command is used if the source language being edited is in Fortran format.   It will cause the Fortran source language stored on the drum to be compiled into symbolic machine language and saved on a different area on the drum.   The Editor can assemble this (or possibly modify it) and the rest of the operation can proceed as described above.   In this system all Fortran subroutines must be compiled and stored individually on the drum before execution can begin.   That is, a Fortran main and a subroutine cannot be compiled and executed as a unit.

The fourth program, Drum Program Store, takes the assembled output from core and puts it on the drum — in a permanent file if this is to be a system program, or a temporary file for debugging, where the resident loader can fetch and store it in its proper place in core and call any library subroutines, if needed.   In addition, there are several programs dedicated to the maintenance of this system.

Of this software package, only the Fortran IV compiler and the new Lincoln Data Analysis Console have yet to be completed. The compiler has been subcontracted. Work on the new console has just been started. The old console as described in TN 1968-14 is being used until the new system is ready.

P. Fleck

REFERENCES

1. T. Utsu, Geophys. Bull. Hokkaido Univ. 13, 99-103 (1965).

2. K. Aki, Bull. Earthquake Res. Inst. 43, 237-239 (1965).

3. P. W. Pomeroy, H. N. Pollack and M. A. Levy, "Seismicity Movies of the Circum-Pacific Belt, 1961 − 1968," presented at the 1969 Annual Meeting of the Seismological Society of America, St. Louis, Missouri.

4. V. I. Tatarskii, Wave Propagation in a Turbulent Medium (McGraw-Hill, New York 1961).

5. D. L. Fried, "Optical Heterodyne Detection of an Atmospherically Distorted Signal Wave Front," Proc. IEEE 55, 57-67 (January 1967).

6. D. L. Fried, "Atmospheric Modulation Noise in an Optical Heterodyne Receiver," IEEE J. Quan. Electron. QE-3, 213 (June 1967).

7. D. A. de Wolfe, J. Opt. Soc. Am. 58, 461-66 (1968).

DOCUMENT CONTROL DATA - R&D

(Security classification of title, body of abstract and indexing annotation must be entered when the overall report is classified)

1. ORIGINATING ACTIVITY *(Corporate author)*	2a. REPORT SECURITY CLASSIFICATION
Lincoln Laboratory, M.I.T.	Unclassified
	2b. GROUP
	None

3. REPORT TITLE

Semiannual Technical Summary Report to the Advanced Research Projects Agency
on Seismic Discrimination

4. DESCRIPTIVE NOTES *(Type of report and inclusive dates)*
Semiannual Technical Summary Report — 1 January to 30 June 1969

5. AUTHOR(S) *(Last name, first name, initial)*

Green, Paul E., Jr.

6. REPORT DATE	7a. TOTAL NO. OF PAGES	7b. NO. OF REFS
30 June 1969	36	15

8a. CONTRACT OR GRANT NO.	9a. ORIGINATOR'S REPORT NUMBER(S)
AF 19(628)-5167	Semiannual Technical Summary
b. PROJECT NO.	(30 June 1969)
ARPA Order 512	
c.	9b. OTHER REPORT NO(S) *(Any other numbers that may be assigned this report)*
d.	ESD-TR-69-159

10. AVAILABILITY/LIMITATION NOTICES

This document has been approved for public release and sale; its distribution is unlimited.

11. SUPPLEMENTARY NOTES	12. SPONSORING MILITARY ACTIVITY
None	Advanced Research Projects Agency, Department of Defense

13. ABSTRACT

Seismic source identification work during this reporting period has emphasized continued studies of short-period discriminants; in particular, the physical sources of some of the spectral effects observed, attempts to exploit arrays of several thousand kilometers' aperture, and a probabilistic model of the two currently most promising discriminants.

14. KEY WORDS

seismic array	seismometers	seismology